Journal of Nonlinear Modeling and Analysis
Volume 8, Number 2, April 2026, 520–550
https://global-sci.com/jnma
DOI:10.12150/jnma.2026.520

Homotopy Analysis Method on Listeria Infection Model Caused by Pre-Cooked Package Food

Sachin K N[1], Mallanagoud Mulimani[2,†], Kumbinarasaiah S[1], Suguntha Devi K[1] and Lavanya N[3]

Received 22 February 2025; Accepted 29 May 2025

Abstract In this study, the Listeria infection model involving the fractional derivatives in the Caputo sense is considered and studied through two different techniques called the Homotopy analysis method (HAM) and Runge-Kutta 4^{th} order (RK4) method. HAM is a semi-analytical approach, and the RK4 method is a numerical method proposed for solving fractional order systems of ordinary differential equations (ODEs). We have developed a semi-analytical solution in terms of a series of polynomials by HAM and a numerical solution by the RK4 method for the model. First, we solved the model through HAM by choosing the preferred control parameter and also applied the RK4 method. The model solved by projected methods is compared with the NDSolver solution. The nature of the model is analyzed using different parameters, and the calculations are performed using Mathematica software. The obtained results are expressed in graphs and tables.

Keywords Homotopy analysis method, Runge-Kutta method, Caputo derivative, Listeria infection model, convergence

MSC(2010) 26A33, 34A08, 34A30, 65H20, 65L06

1. Introduction

Differential equations have numerous applications, such as describing objects' motion, including projectiles, oscillations, and collisions in classical mechanics; the behavior of electric circuits and electromagnetic waves in electromagnetism, and calculating an item's temperature over time using Newton's law of cooling. Population increase and saturation are modeled using the logistic equation. The SIR model comprehends the transmission of illnesses. The Lorenz system simulates how air circulation and fluid convection behave. We can compute acceleration and velocity. Design and enhance control systems for processes using electricity, mechanical, and chemical elements. Signal handling in audio, picture, and video processing, analyzes and filters signals. Population dynamics examines how different species interact, considering theories of competition and predator-prey relationships. The

[†]the corresponding author.
Email address: mallanagoudmulimani@gmail.com; mulimani@kbn.university (Mallanagoud Mulimani)
[1]Department of Mathematics, Bangalore University, Bengaluru, 560056, India
[2]Department of Applied Sciences, Faculty of Engineering and Technology, Khaja Bandanawaz University, Kalaburagi, 585104, India
[3]Department of Mathematics, PG Centre Ramanagara, Bangalore University, Ramanagara, India

study of epidemiology models the transmission of illnesses, taking into account the effects of immunization and therapeutic approaches. Lotka-Volterra formulae simulate the behavior of predator-prey networks. Hodgkin-Huxley formulae explain how nerve impulses in neurons behave.

Fractional calculus (FC) is a branch of classical calculus that deals with non-integer (fractional) order differentiation and integration procedures. The notion of fractional operators was created nearly concurrently with the introduction of classical operators. In 1695, renowned scientists like the Marquis de l'Hospital and G. W. Leibniz expanded the definition of the semi-derivative. As a result, numerous prominent mathematicians, such as Letnikov, Grünwald, Riemann, Laplace, Liouville, and Euler, became interested in this topic. The theory of FC has advanced quickly since the 19th century, primarily serving as a basis for several practical fields, such as fractional dynamics, fractional differential equations, and fractional geometry. These days, FC has many different uses. It is reasonable to state that practically every field of contemporary science and engineering, in general, is impacted by the schemes and tools of FC. Bioengineering, mechanical and electrical engineering, control theory, robotics, statistical and chemical physics, optics, acoustics, viscoelasticity, rheology, and other fields, for instance, have numerous and productive uses. In general, one may contend that processes in the real world are fractional order systems. These new fractional-order models are frequently more accurate than integer-order ones, meaning they have more degrees of freedom than the corresponding classical model. This is the primary factor contributing to the success of FC applications. This topic is fascinating because fractional integrals and derivatives are non-integer or non-local quantities. To describe the non-local and spread effects frequently found in technological and natural events, all fractional operators take into account the complete history of the process under consideration. As a result, FC is a great collection of instruments for characterizing the memory and inherited characteristics of different materials and processes. The articles [1, 2] provide a clear explanation of the FC.

Listeriosis, or Listeria infection, is caused by the bacterium Listeria monocytogenes. This is a dangerous disease that primarily affects older people, infants, expectant mothers, and persons with weakened immune systems. Numerous environmental elements contain Listeria bacteria, including soil, water, and some animals. Food contamination is a common way for people to get infected with Listeria. Common sources of disease include soft cheeses, hot dogs, deli meats, unpasteurized dairy products, and smoked fish. These foods, even when refrigerated, can harbour Listeria [3].

Muscle aches, headaches, nausea, fever, and diarrhea are just a few symptoms that can be produced by listeriosis [4]. Meningitis, an inflammation of the membranes surrounding the spinal cord and brain, and septicemia, a blood infection, are among the complications that might arise from severe circumstances [5]. Due to the possibility of miscarriage, death, early delivery, or illness in the unborn child, some populations—including pregnant women—are more vulnerable to severe listeriosis [6]. Individuals with compromised immune systems with organ transplants, AIDS/HIV, cancer, or older people may be at a higher risk.

Antibiotics are a treatment option for listeriosis. If you think you may have a Listeria infection, you should see a doctor every once, especially if you are in a high-risk category. Adopting sensible food safety practices is essential to prevent Listeria contamination. Fruits and vegetables should be cleaned, dairy products should

not be consumed raw or unpasteurized, meat and poultry should be cooked before eating, and food should be handled carefully to avoid cross-contamination [7]. When a pregnant woman exhibits symptoms of a Listeria infection, she should contact a doctor right away since receiving treatment early on can protect the unborn child as well as the mother [8, 9].

To prevent and control listeriosis infection, some mathematical models were investigated. Recently, Massia [11] investigated the impact of freezing on Listeria monocytogenes in hot dog sausages, and Asamoah et al. [10] provided a fractional ordered listeriosis model employing two kernels. In the presence of bovine milk products, Zhang et al. [12] provided survival and prediction modeling of Listeria monocytogenes in circumstances approximated by the human stomach.

Mathematical modeling is a useful and adaptable tool in many fields that helps us investigate, evaluate, and solve challenging real-world issues. It is essential for knowledge advancement, better decision-making, and innovation in theoretical and applied fields of study [13]. Its significance comes from its capacity to use mathematical equations to describe and analyze complicated real-world occurrences, which may yield insightful conclusions, insightful forecasts, and useful solutions. Drug discovery [16], treatment optimization [15], and illness spread prediction [14] are all areas where mathematical modeling is heavily utilized in the healthcare industry. It is essential to systems biology [19], pharmacokinetics [18], and epidemiology [17].

Because they can explain complex behaviors and memory effects in a wide range of scientific and technical domains, fractional-order mathematical models are helpful supplements to conventional integer-order models [20–22]. Their capacity to record long-range and non-local interactions in numerous systems has led to an increase in focus in recent years. Working with fractional-order mathematical models presents challenges for numerical methods, mathematical analysis, and result interpretation; proper simulation and solution of these models frequently call for specialized software and mathematical methods.

Mathematical fractional order models find use in many domains, such as Chen et al. [23] covered a model of the environment and economy at fractional order. Using a computationally supervised neural network process to a fractional mathematical model was proposed by Mukdasai et al. [24]. Veeresha et al. [25] presented a fractional system of the harmful interactions between phytoplankton and zooplankton, while Bilgil et al. [26] used vaccinated and infected SARS-CoV-2 compartments to develop a fractional-order model, Khirsariya et al. [27, 28] explained a fractional diabetes model, an age-specific, the smoke epidemic model in fractional order was presented by Addai et al. [29], and the model of fractional omicron variant described by Sharma et al. [30].

The semi-analytical method, HAM, is used to solve differential equations, including ODEs, PDEs, and fractional order differential equations. HAM is independent of small and big parameters, unlike perturbation methods that rely on them. The choice of auxiliary function, linear operator, and control convergence parameter is entirely up to us. This approach typically resolves highly nonlinear differential equations [31]. HAM is a semi-analytical method that generates a series of concurrent linear equations from a nonlinear one by using homotopy, or the deformation of one continuous function into another, to solve nonlinear or partial differential equations.

Liao created HAM initially in 1992, and it underwent additional changes in 1997 with the addition of the auxiliary parameter h. This non-zero parameter gives the

series control over its convergence. We are free to select the auxiliary linear operator, the convergence control parameter h, and the initial approximation of the solution because HAM is predicated on the idea of homotopy [32]. The HAM is a potent and user-friendly analytical tool for general nonlinear problems that is refined and explained in detail using a typical nonlinear problem. Two proposed rules that simplify using the HAM in science and engineering are the rule of coefficient ergodicity and the rule of solution expression. Both of these rules have significant roles in the framework of the HAM. For the first time, an explicit analytic solution is provided along with recursive coefficient formulas. Liao introduced HAM, an analytical approximation method, for highly nonlinear problems in his Ph.D. thesis in 1992. The HAM can always be used to convert a nonlinear problem into an infinite number of linear sub-problems, unlike perturbation techniques, which depend on physical parameters of any size. Secondly, the HAM offers us a practical means of ensuring the convergence of the solution series, which makes it valid even in cases where nonlinearity becomes quite strong, in contrast to all other analytical techniques. Furthermore, because homotopy in topology allows us to have a great deal of flexibility in determining the type of linear subproblems, the solution's base function, the starting estimate, and other factors, complicated nonlinear ODEs and PDEs can frequently be solved in an easy-to-understand manner. So, to address extremely nonlinear problems in science, finance, and engineering, the HAM offers us a helpful tool [33]. The HAM has made acquiring semi-analytical solutions to a wide range of nonlinear differential equations possible. To guarantee the convergence of the solutions and to raise the rate and region of convergence, one can choose auxiliary functions, operators, and parameters with a considerable deal of freedom with this method.

The paper is organized as follows. Section 2 introduces the definitions of fractional calculus and theorems on convergence analysis. Section 3 discusses the method for solving differential equations. Section 4 describes the formulation of the model. Section 5 shows the algorithm for the model. The results from the numerical experiments are presented in Section 6, accompanied by illustrative figures and informative tables that demonstrate the proposed methodology's effectiveness. Finally, Section 7 concludes by summarising the key research findings and outlining potential avenues for future investigation.

2. Preliminaries

Definition 2.1. The fractional derivative of $f(x)$ in the Caputo sense is defined as:

$$D^{\alpha} f(x) = I^{n-\alpha} D^{n} f(x) = \frac{1}{\Gamma(n-\alpha)} \int_{0}^{x} (x-t)^{x-\alpha-1} f^{n}(t) dt, \tag{2.1}$$

for $n-1 < \alpha \leq n, n \in \mathbb{N}, x > 0, f \in C_{-1}^{n}$ [38].

Definition 2.2. The fractional integration of x^n in the Caputo sense is given by

$$I^{\alpha} x^{n} = \frac{x^{n+\alpha} \Gamma(1+n)}{\Gamma(1+n+\alpha)}, \tag{2.2}$$

for $n-1 < \alpha \leq n, n \in \mathbb{N}, x > 0$.

Theorem 2.1. *As long as the series* $v_i(y) = \sum_{m=0}^{m} v_{i_m}(y)$ *converges, it must be the exact solution of* (3.10)*, where* $v_{i_m}(y)$ *is governed by the* m^{th} *order deformation equation [40].*

Theorem 2.2. *Let* $\psi_0, \psi_1, \psi_2, \ldots$ *be the components of solution of equation* (3.10)*. The series solution* $\sum_{k=0}^{\infty} \psi_k(t)$ *converges if* $\exists\ 0 < \gamma < 1$ *such that* $||\psi_{k+1}|| \leq \gamma ||\psi_k||$*,* $\forall\ k \geq k_0$ *for some* $k_0 \in \mathbb{N}$ *[34].*

Theorem 2.3. *Assume that the series solution* $\sum_{k=0}^{\infty} \psi_k(t)$ *is convergent to the solution* $y(t)$*, if the truncation series* $\sum_{k=0}^{m} \psi_k(t)$ *is the approximation to the solution* $v_i(y)$*, then the maximum absolute truncation error is calculated as,* $||v_i(y) - \sum_{k=0}^{m} \psi_k(t)|| \leq \frac{1}{1-\gamma}\ \gamma^{m+1}\ ||\psi_0(t)||$ *[34].*

3. Method of solution

3.1. Homotopy analysis method for ODEs

Consider the ODE with different physical conditions,

$$\mathscr{M}[v(y)] = 0, y \geq 0, \tag{3.1}$$

where $\mathscr{M}$ is the differential operator, and v(y) is the function to be determined.

Let $v_0(y)$ be the initial approximation to the actual solution of (3.1). The zeroth deformation equation is constructed using the auxiliary function $\mathscr{H}$(y) $(\neq 0)$ and auxiliary parameter h $(\neq 0)$ as [35],

$$(1-q)\mathscr{S}[\psi(y;q) - v_0(y)] = qh\mathscr{H}(y)\mathscr{M}[\psi(y;q)], \tag{3.2}$$

where $\psi(y;q)$ is an unknown function, $\mathscr{S}$ is a linear operator.

When $q = 0$, (3.2) becomes $\psi(y;0) = v_0\ (y)$ and at $q = 1$, (3.2) becomes $\psi(y;1) = v(y)$. So as q varies from 0 to 1, the function $\psi(y;q)$ varies from the initial approximation $v_0(y)$ to the actual solution $v(y)$. Defining the m^{th} order deformation derivatives,

$$v_m(y) = \frac{1}{m!}\frac{\partial^m \psi(y;q)}{\partial q^m}. \tag{3.3}$$

Expanding $\psi(v;q)$ using the Taylor series with respect to (w.r.t.) q, we get,

$$\psi(y;q) = v_0(y) + \sum_{m=1}^{\infty} v_m(y) q^m. \tag{3.4}$$

As we know, $\psi(y;q)$ becomes the desired solution at $q = 1$.

At $q = 1$, equation (3.4) becomes,

$$\psi(y;1) = v(y) = v_0(y) + \sum_{m=1}^{\infty} v_m(y). \tag{3.5}$$

Similarly, the deformation equation of m^{th} order is obtained as,

$$\mathscr{S}[v_m(y) - \chi_m v_{m-1}(y)] = h\mathscr{H}(y)\mathscr{R}_m(v_{m-1}(y)), \tag{3.6}$$

where,

$$\chi_m = \begin{cases} 0 & \text{if} \quad m \leq 1, \\ 1 & \text{if} \quad m \geq 1. \end{cases} \tag{3.7}$$

$$\mathscr{R}_m(v_{m-1}(y)) = \frac{1}{(m-1)!} \frac{\partial^{m-1}[\mathscr{M}[\psi(y;q)]]}{\partial q^{m-1}}. \tag{3.8}$$

Thus $v_1(y)$, $v_2(y)$, $v_3(y), \ldots$ can be attained by solving equation (3.6).

The m^{th} order approximation of $v(y)$ [36] is given by

$$v(y) = \sum_{m=0}^{m} v_m(y). \tag{3.9}$$

(3.9) is the semi-analytical solution of (3.1).

3.2. Homotopy analysis method for system of ODEs

Consider the system of stiff ODEs with different physical conditions [37],

$$[v_i'(y)] = g_i(y, v_1, v_2, \ldots, v_n), \qquad i = 1, 2, 3, \ldots, n, \quad y \geq 0 \tag{3.10}$$

subject to the condition:

$$v_i(0) = a_i, \qquad i = 1, 2, 3, \ldots, n. \tag{3.11}$$

Let $v_{i_0}(y)$, $i = 1, 2, 3, \ldots, n.$ be the initial approximation to the actual solution of (3.10). The Zeroth deformation equations take the auxiliary function $\mathscr{H}(y)$ $(\neq 0)$ and auxiliary parameter h $(\neq 0)$ as [35, 39],

$$(1-q)\mathscr{S}_i[\psi_i(y;q) - v_{i_0}(y)] = qh\mathscr{H}(y)\mathscr{M}_i[\psi_i(y;q)], \quad i = 1, 2, 3, \ldots, n, \tag{3.12}$$

subject to the conditions:

$$\psi_i(0;q) = a_i, \quad i = 1, 2, 3, \ldots, n, \tag{3.13}$$

where, $\psi_i(y;q)$ are unknown functions, and $\mathscr{S}_i$ are the linear operators.

When $q = 0$, (3.12) becomes, $\psi_i(y;0) = v_{i_0}(y)$ and at $q = 1$, (3.12) becomes, $\psi_i(y;1) = v_i(y)$. So as q varies from 0 to 1, the function $\psi_i(y;q)$ varies from initial approximation $v_{i_0}(y)$ to the actual solution $v_i(y)$, $i = 1, 2, 3, \ldots, n$. Defining the m^{th} order deformation derivatives,

$$v_{i_m}(y) = \frac{1}{m!} \frac{\partial^m \psi_i(y;q)}{\partial q^m}, \quad i = 1, 2, 3, \ldots, n. \tag{3.14}$$

Expanding $\psi_i(y;q)$ using Taylor series w.r.t. q, $\quad i = 1, 2, 3, \ldots, n$, we get,

$$\psi_i(y;q) = v_{i_0}(y) + \sum_{m=1}^{\infty} v_{i_m}(y) q^m \quad i = 1, 2, 3, \ldots, n. \tag{3.15}$$

As we know at $q = 1$, $\psi_i(y;q)$ becomes the required solution, and equation (3.15) at $q = 1$ becomes,

$$\psi_i(y;1) = v_i(y) = v_{i_0}(y) + \sum_{m=1}^{\infty} v_{i_m}(y), \quad i = 1, 2, 3, \ldots, n. \tag{3.16}$$

Similarly, the m^{th} order deformation is given by

$$\mathscr{S}[v_{i_m}(y) - \chi_m v_{i_{m-1}}(y)] = h\mathscr{H}(y)R_{i,m}(v_{i_{m-1}}(y)), \quad i = 1, 2, 3, \ldots, n, \tag{3.17}$$

where,

$$\chi_m = \begin{cases} 0 & \text{if} \quad m \leq 1, \\ 1 & Otherwise. \end{cases} \tag{3.18}$$

$$R_{i,m}(v_{i_{m-1}}(y)) = \frac{1}{(m-1)!}\frac{\partial^{m-1}[\mathscr{M}[\psi_i(y;q)]]}{\partial q^{m-1}}, \quad i = 1, 2, 3, \ldots, n. \tag{3.19}$$

Thus $v_{i_1}(y)$, $v_{i_2}(y)$, $v_{i_3}(y), \ldots$ can be obtained by solving equation (3.17). The m^{th} order approximation of $v_i(y)$ [41] is given by

$$v_i(y) = \sum_{m=0}^{m} v_{i_m}(y). \tag{3.20}$$

(3.20) is the semi-analytical solution of (3.10).

4. Model formulation

The mathematical model of Listeria infection contains three layers: pre-cooked package food, the Listeria population in the environment, and the human population. Pre-cooked packaged food products are divided into two classes: uncontaminated food F_u and contaminated food F_c. So, the total food products are $F = F_u + F_c$.

Table 1. The Listeria infection model presented is described using parameters.

Notations	Description	Values
K_c	Carrying Capacity of L_c	0.008
Λ_2	Uncontaminated to contaminated food convergence rate	0.01
μ_2	Uncontaminated food production rate	0.01
ρ_1	Immunity lost rate	0.1
β	Net growth rate of L_c	0.01
γ	Recovery rate	0.05
Λ_1	Environmental transmission rate	0.005
μ_1	Natural death rate	$\frac{1}{65\times360}$

The assumed constant rate of production of uncontaminated food is μ_2, and the convergence rate from uncontaminated food to contaminated food is Ω_2 due to bacteria from the atmosphere and the distribution process of the factory. Food products have a removal rate of μ_f. We assumed that the growth of the bacteria was logistical. The net growth rate of class L_c of Listeria monocytogenes bacteria is β with the carrying capacity $0 \leq K_c \leq 1$.

To study the Listeria infection, three standard classes of the SIR model are identified for the entire human population $N(t)$: susceptible class $S(t)$, infected class $I(t)$, and recovered class $R(t)$. Therefore, at any given time t, the entire population $N(t)$ is provided by

$$N(t) = S(t) + I(t) + R(t).$$

The class of susceptible humans expands at the rate $\mu_1 N(t)$ with μ_1 also the mortality rate of each class of population and Ω_1 is the transmission rate from susceptible human to infected human due to consumption of contaminated food and by Listeria bacteria from the environment. Infected humans are recovered with the rate α. We considered that the recovered human can become susceptible with rate ρ due to low immunity.

All parameters required to create the Listeria infection model are listed in Table 1 along with a thorough description and values. The corresponding system of ODEs is [42]:

$$\left.\begin{aligned}
\tfrac{dS}{dt} &= \mu_1 N + \rho R - (\Lambda_1 + \mu_1)S,\\
\tfrac{dI}{dt} &= \Lambda_1 S - (\gamma + \mu_1)I,\\
\tfrac{dR}{dt} &= \gamma I - (\rho + \mu_1)R,\\
\tfrac{dL_c}{dt} &= \beta L_c(1 - \tfrac{L_c}{K_c}),\\
\tfrac{dF_c}{dt} &= \Lambda_2 F_u - \mu_2 F_c,\\
\tfrac{dF_u}{dt} &= \mu_2 F - (\Lambda_2 + \mu_2)F_u.
\end{aligned}\right\} \tag{4.1}$$

After applying the Caputo fractional derivative to the above system [42], we get

$$\left.\begin{aligned}
{}^{C}D_t^{\alpha} S(t) &= \mu_1 N + \rho R - (\Lambda_1 + \mu_1)S,\\
{}^{C}D_t^{\alpha} I(t) &= \Lambda_1 S - (\gamma + \mu_1)I,\\
{}^{C}D_t^{\alpha} R(t) &= \gamma I - (\rho + \mu_1)R,\\
{}^{C}D_t^{\alpha} L_c(t) &= \beta L_c(1 - \tfrac{L_c}{K_c}),\\
{}^{C}D_t^{\alpha} F_c(t) &= \Lambda_2 F_u - \mu_2 F_c,\\
{}^{C}D_t^{\alpha} F_u(t) &= \mu_2 F - (\Lambda_2 + \mu_2)F_u.
\end{aligned}\right\} \tag{4.2}$$

5. Solution of Listeria infection model

Consider the system of ODEs defined in Eq. (4.1) with the initial condition,

$$S_0(t)=600,\ I_0(t)=20,\ R_0(t)=10,\ L_{c_0}(t)=0.2ln(10),\ F_{c_0}(t)=300,\ F_{u_0}(t)=10. \tag{5.1}$$

To solve Eq. (4.1) by HAM, assume that

$$L = D^{\alpha} \text{ and } H(t) = 1. \tag{5.2}$$

We construct the zeroth-order deformation equations,

$$\left.\begin{array}{l}(1-q)L[\phi_1(t;q)-S_0(t)]=qhN[\phi_i(t;q)],\\(1-q)L[\phi_2(t;q)-I_0(t)]=qhN[\phi_i(t;q)],\\(1-q)L[\phi_3(t;q)-R_0(t)]=qhN[\phi_i(t;q)],\\(1-q)L[\phi_4(t;q)-L_{c_0}(t)]=qhN[\phi_i(t;q)],\\(1-q)L[\phi_5(t;q)-F_{c_0}(t)]=qhN[\phi_i(t;q)],\\(1-q)L[\phi_6(t;q)-F_{u_0}(t)]=qhN[\phi_i(t;q)].\end{array}\right\}\quad for\quad i=1(1)6. \tag{5.3}$$

Differentiating the zeroth-order deformation Eq. (5.3) m times with respect to q, and finally dividing by $m!$, we obtain the m^{th}-order deformation equations as

$$\left.\begin{array}{l}L[S_m(t)-\chi_m S_{m-1}(t)]=h\overrightarrow{R}_m(S_m(t)),\\L[I_m(t)-\chi_m I_{m-1}(t)]=h\overrightarrow{R}_m(I_m(t)),\\L[R_m(t)-\chi_m R_{m-1}(t)]=h\overrightarrow{R}_m(R_m(t)),\\L[L_{c_m}(t)-\chi_m L_{c_{m-1}}(t)]=h\overrightarrow{R}_m(L_{c_m}(t)),\\L[F_{c_m}(t)-\chi_m F_{c_{m-1}}(t)]=h\overrightarrow{R}_m(F_{c_m}(t)),\\L[F_{u_m}(t)-\chi_m F_{u_{m-1}}(t)]=h\overrightarrow{R}_m(F_{u_m}(t)),\end{array}\right\} \tag{5.4}$$

with,

$$S_m(0)=0,\ I_m(0)=0,\ R_m(0)=0,\ L_{c_m}(0)=0,\ F_{c_m}(0)=0,\ F_{u_m}(0)=0, \tag{5.5}$$

where,

$$\left.\begin{array}{ll}\overrightarrow{R}_m(S_m(t))= & D^\alpha S_{m-1}(t)-\mu_1 N-\rho R_{m-1}(t)+(\Lambda_1+\mu_1)S_{m-1}(t),\\ \overrightarrow{R}_m(I_m(t))= & D^\alpha I_{m-1}(t)-\Lambda_1 S_{m-1}(t)+(\gamma+\mu_1)I_{m-1}(t),\\ \overrightarrow{R}_m(R_m(t))= & D^\alpha R_{m-1}(t)-\gamma I_{m-1}(t)+(\rho+\mu_1)R_{m-1}(t),\\ \overrightarrow{R}_m(L_{c_m}(t))= & D^\alpha L_{c_{m-1}}(t)-\beta L_{c_{m-1}}(t)+\frac{\beta}{K_m}\sum_{j=0}^{m-1}L_{c_j}(t)L_{c_{m-1-j}}(t),\\ \overrightarrow{R}_m(F_{c_m}(t))= & D^\alpha F_{c_{m-1}}(t)-\Lambda_2 F_{u_{m-1}}(t)+\mu_2 F_{c_{m-1}}(t),\\ \overrightarrow{R}_m(F_{u_m}(t))= & D^\alpha F_{u_{m-1}}(t)-\mu_2 F+(\Lambda_2+\mu_2)F_{u_{m-1}}(t).\end{array}\right\} \tag{5.6}$$

Solving equations (5.6) for $m\geq 1$ and substituting the values of the parameters as given in Table 1 we get,

$$\left.\begin{array}{ll}S_m(t)= & \chi_m S_{m-1}(t)+h\int\big(D^\alpha S_{m-1}(t)-2.6\times10^{-2}-0.1R_{m-1}(t)\\ & +5.04\times10^{-3}S_{m-1}(t)\big)dt,\\ I_m(t)= & \chi_m I_{m-1}(t)+h\int\big(D^\alpha I_{m-1}(t)-0.005S_{m-1}(t)+0.05I_{m-1}(t)\big)dt,\\ R_m(t)= & \chi_m R_{m-1}(t)+h\int\big(D^\alpha R_{m-1}(t)-0.05I_{m-1}(t)+0.1R_{m-1}(t)\big)dt,\\ L_{c_m}(t)= & \chi_m L_{c_{m-1}}(t)+h\int\big(D^\alpha L_{c_{m-1}}(t)-0.01L_{c_{m-1}}(t)\\ & +1.25\sum_{j=0}^{m-1}L_{c_j}(t)L_{c_{m-1-j}}(t)\big)dt,\\ F_{c_m}(t)= & \chi_m F_{c_{m-1}}(t)+h\int\big(D^\alpha F_{c_{m-1}}(t)-0.01F_{u_{m-1}}(t)+0.01F_{c_{m-1}}(t)\big)dt,\\ F_{u_m}(t)= & \chi_m F_{u_{m-1}}(t)+h\int\big(D^\alpha F_{u_{m-1}}(t)-3.1+0.02F_{u_{m-1}}(t)\big)dt.\end{array}\right\} \tag{5.7}$$

For $m = 1$, Eq. (5.7) becomes,

$$\begin{aligned} S_1(t) =&\chi_1 S_0(t) + h\int \big(D^\alpha S_0(t) - 2.6\times 10^{-2} - 0.1R_0(t) + 5.04\times 10^{-3}S_0(t)\big)dt,\\ =&h\int \big(0 - 2.6\times 10^{-2}(10) + 5.04\times 10^{-3}(600)\big)dt,\\ =&1.998ht + c_1. \end{aligned}$$

Using the condition from Eq. (5.5), we get $c_1 = 0$.
$\therefore\ S_1(t) = 1.998ht.$

$$\begin{aligned} I_1(t) =&\chi_1 I_0(t) + h\int \big(D^\alpha I_0(t) - 0.005S_0(t) + 0.05I_0(t)\big)dt,\\ =&h\int \big(0 - 0.005(600) + 0.05(20)\big)dt,\\ =&-2ht + c_2. \end{aligned}$$

Using the condition from Eq.(5.5), we get $c_2 = 0$.
$\therefore\ I_1(t) = -2ht.$

$$\begin{aligned} R_1(t) =&\chi_1 R_0(t) + h\int \big(D^\alpha R_0(t) - 0.05I_0(t) + 0.1R_0(t)\big)dt,\\ =&h\int \big(0 - 0.05(20) + 0.1(10)\big)dt,\\ =&0 + c_3. \end{aligned}$$

Using the condition from Eq. (5.5), we get, $c_3 = 0$.
$\therefore\ R_1(t) = 0$.

$$\begin{aligned} L_{c_1}(t) =&\chi_1 L_{c_0}(t) + h\int \big(D^\alpha L_{c_0}(t) - 0.01L_{c_0}(t) + 1.25\sum_{j=0}^{0} L_{c_j}L_{c_j}\big)dt,\\ =&h\int \big(0 - 0.01(0.460517018) + 1.25(0.460517018)^2\big)dt,\\ =&0.2604ht + c_4. \end{aligned}$$

Using the condition from Eq. (5.5), we get, $c_4 = 0$.
$\therefore\ L_{c_1}(t) = 0.2604ht.$

$$\begin{aligned} F_{c_1}(t) =&\chi_1 F_{c_0}(t) + h\int \big(D^\alpha F_{c_0}(t) - 0.01F_{u_0}(t) + 0.01F_{c_0}(t)\big)dt,\\ =&h\int \big(0 - 0.01(10) + 0.01(300)\big)dt,\\ =&2.9ht + c_5. \end{aligned}$$

Using the condition from Eq. (5.5), we get, $c_5 = 0$.
$\therefore\ F_{c_1}(t) = 2.9ht.$

$$F_{u_1}(t) =\chi_1 F_{u_0}(t) + h\int \big(D^\alpha F_{u_0}(t) - 3.1 + 0.02F_{u_0}(t)\big)dt,$$

$$=h\int\big(0-3.1+0.02(10)\big)dt,$$
$$=-2.9ht+c_6.$$

Using the condition from Eq. (5.5), we have, $c_6=0$.
$\therefore F_{u_1}(t)=-2.9ht.$

Similarly, for $m=2$, we get

$$S_2(t)=1.972ht+1.998h^2t+0.01\frac{h^2t^2}{2}.$$
$$I_2(t)=-2ht-2h^2t-0.1099\frac{h^2t^2}{2}.$$
$$R_2(t)=-0.1\frac{h^2t^2}{2}.$$
$$L_{c_2}(t)=0.2604ht+0.2604h^2t-2.604\times10^{-3}\frac{h^2t^2}{2}+0.01797\frac{h^3t^3}{3}.$$
$$F_{c_2}(t)=2.9ht+2.9h^2t+0.058\frac{h^2t^2}{2}.$$
$$F_{u_2}(t)=-6ht-2.9h^2-0.058\frac{h^2t^2}{2}.$$

From Eq. (3.20), the solutions of Listeria infection model are

$$S(t)=S_0(t)+S_1(t)+S_2(t)+\cdots,$$
$$S(t)=600+1.998ht+1.972ht+1.998h^2t+0.01\frac{h^2t^2}{2}+\cdots,$$
$$I(t)=I_0(t)+I_1(t)+I_2(t)+\cdots,$$
$$I(t)=20-2ht-2ht-2h^2t-0.1099\frac{h^2t^2}{2}+\cdots,$$
$$R(t)=R_0(t)+R_1(t)+R_2(t)+\cdots,$$
$$R(t)=10+0-0.1\frac{h^2t^2}{2}+\cdots,$$

$$L_c(t)=L_{c_0}(t)+L_{c_1}(t)+L_{c_2}(t)+\cdots,$$
$$L_c(t)=0.2ln(10)+0.2604ht+0.2604ht+0.2604h^2t-2.604\times10^{-3}\frac{h^2t^2}{2}+0.01797\frac{h^3t^3}{3}+\cdots.$$
$$F_c(t)=F_{c_0}(t)+F_{c_1}(t)+F_{c_2}(t)+\cdots,$$
$$F_c(t)=300+2.9ht+2.9ht+2.9h^2t+0.058\frac{h^2t^2}{2}+\cdots.$$
$$F_u(t)=F_{u_0}(t)+F_{u_1}(t)+F_{u_2}(t)+\cdots,$$

$$F_u(t) = 10 - 2.9ht - 6ht - 2.9h^2 - 0.058\frac{h^2t^2}{2} + \cdots .$$

We have used the *Mathematica 13.2* software to compute the above solutions and calculated up to $m = 15$ terms, setting $h = -1$. The obtained results are discussed below.

The general algorithm for HAM:

1. Consider the problem with boundary conditions.
2. Define the zeroth order deformation equations.
3. Verify the boundary conditions for the zeroth order deformation equations.
4. Generate the higher-order deformation equations.
5. Solve the higher-order deformation equations pointwise.
6. Construct the approximate solution.
7. Determine the optimal auxillary parameter by h-curves.
8. Iterate and refine the obtained solution.

6. Numerical results and discussion

Additionally, the RK4 method is used to resolve the above system of ODEs. Graphs and tables are used to explain the results that were obtained. Tables 2 and 3 give the values of $S(t)$, for integer and non-integer values of α. The geometrical comparison of the HAM, RK4, and NDSolve solutions of $S(t)$ is shown in Figure 1. Figure 2 displays the error analysis of the HAM and RK4 solution for $S(t)$. The graphical depiction of the HAM solution with various values of α of $S(t)$ is shown in Figure 3.

Tables 4 and 5 display the computed values of $I(t)$ for both integer and fractional values of α. Figure 4 provides a geometric comparison of the solutions obtained using HAM, RK4, and ND Solve for $I(t)$. The error analysis between the HAM and RK4 methods for $I(t)$ is presented in Figure 5. Furthermore, Figure 6 illustrates the graphical representation of the HAM solution for $I(t)$ across different values of α.

Tables 6 and 7 provide the values of $R(t)$ for integer and non-integer values of α. Figure 7 compares the geometrical solutions of $R(t)$ from HAM, RK4, and NDSolve. Figure 8 shows an error analysis of the HAM and RK4 solutions for $R(t)$. Figure 9 shows a graphical representation of the HAM solution with several α values for $R(t)$.

Tables 8 and 9 provide the values of $L_c(t)$ for integer and non-integer values of α. Figure 10 compares the geometrical solutions of $L_c(t)$ from HAM, RK4, and NDSolve. Figure 11 shows the error analysis of HAM and RK4 solutions for $L_c(t)$. Figure 12 shows a graphical representation of the HAM solution for several α values of $L_c(t)$.

Tables 10 and 11 give the values of $F_c(t)$, for integer and non-integer values of α. The geometrical comparison of the HAM, RK4, and NDSolve solutions of $F_c(t)$ is shown in Figure 13. Figure 14 displays the error analysis of the HAM and RK4 solution for $F_c(t)$. The graphical depiction of the HAM solution with various values of α of $F_c(t)$ is shown in Figure 15.

Tables 12 and 13 illustrate the values of $F_u(t)$ for integer and non-integer values of α. Figure 16 compares the geometrical solutions of $F_u(t)$ from HAM, RK4, and ND Solve. Figure 17 shows an error analysis of the HAM and RK4 solutions for $F_u(t)$. Figure 18 shows a graphical representation of the HAM solution with several α values for $F_u(t)$.

Table 2. Comparison of the HAM and RK4 solutions with NDSolve solution for $\alpha = 1$ of Susceptible class $S(t)$.

t	NDSolve	RK4	HAM	AE by RK4	AE by HAM
0	600	600	600	0	0
1	598.0078932	598.007892	598.0078933	1.2417×10^{-6}	5.8260×10^{-8}
2	596.0348851	596.034882	596.0348845	3.0732×10^{-6}	5.7324×10^{-7}
3	594.0887468	594.088742	594.0887459	4.7881×10^{-6}	8.8810×10^{-7}
4	592.1759904	592.175986	592.1759903	4.4259×10^{-6}	1.2598×10^{-7}
5	590.3020166	590.302011	590.3020165	5.5953×10^{-6}	9.5338×10^{-8}
6	588.4712417	588.471236	588.4712414	5.6775×10^{-6}	2.7757×10^{-7}
7	586.6872173	586.687211	586.6872169	6.3495×10^{-6}	4.4959×10^{-7}
8	584.9527358	584.952730	584.9527357	5.7946×10^{-6}	9.4625×10^{-8}
9	583.2699267	583.269919	583.2699250	7.6517×10^{-6}	1.6517×10^{-6}
10	581.6403337	581.640325	581.6403312	8.6971×10^{-6}	2.4971×10^{-6}

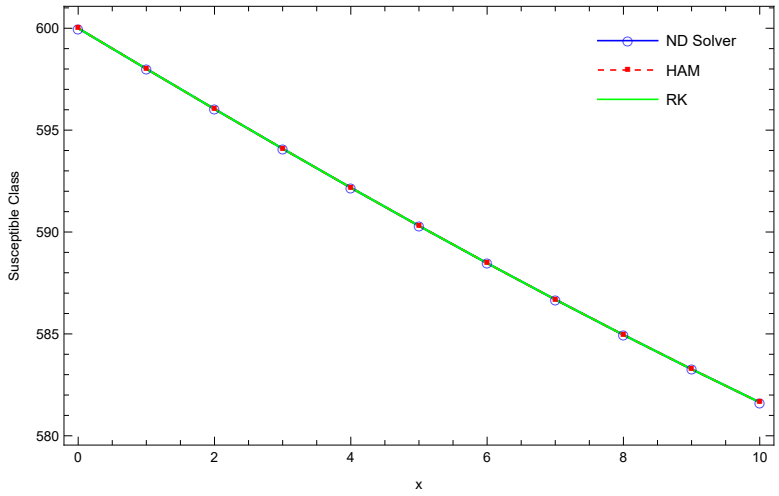

Figure 1. Comparison of the HAM and RK4 solutions with NDSolve solution for $\alpha = 1$ of Susceptible class $S(t)$.

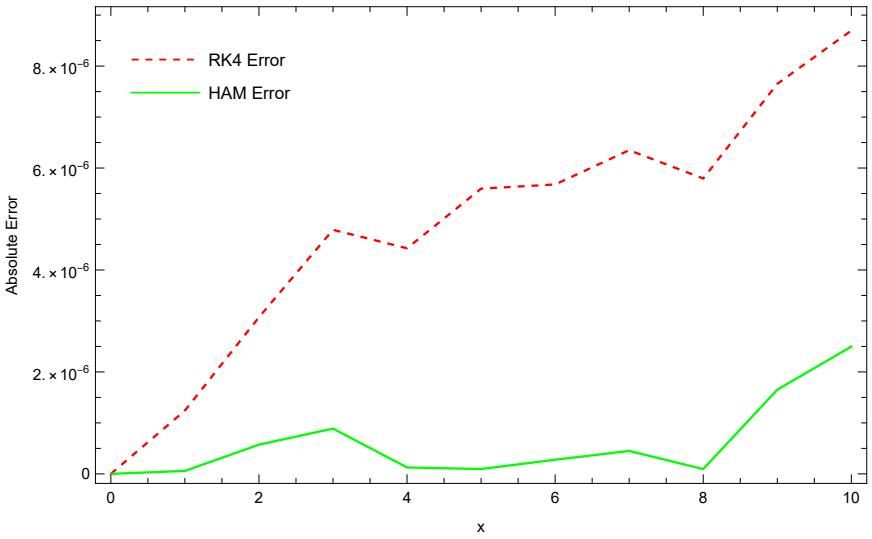

Figure 2. Error analysis of HAM and RK4 solution of Susceptible class $S(t)$.

Table 3. HAM solutions for different fractional values of Susceptible class $S(t)$.

t	$\alpha = 0.2$	$\alpha = 0.4$	$\alpha = 0.6$	$\alpha = 0.8$	$\alpha = 1$
0	600	600	600	600	600
1	597.8440493	597.7660991	597.7776219	597.8641929	598.0078933
2	597.5286073	597.0640377	596.6484665	596.3007766	596.0348845
3	597.3236790	596.5581700	595.7458401	594.9130168	594.0887459
4	597.1683685	596.1492566	594.9678322	593.6365689	592.1759903
5	597.0419247	595.8004218	594.2730257	592.4431476	590.3020165
6	596.9345798	595.4932756	593.6394328	591.3168386	588.4712414
7	596.8408999	595.2171244	593.0536195	590.2474086	586.6872169
8	596.7575292	594.9651210	592.5066187	589.2276856	584.9527357
9	596.6822399	594.7325791	591.9920662	588.2523280	583.2699250
10	596.6134728	594.5161301	591.5052369	587.3171728	581.6403312

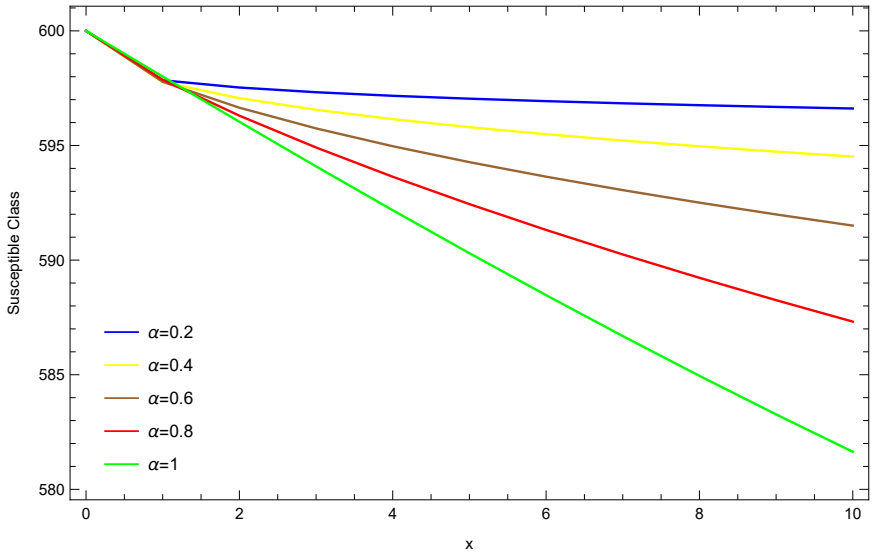

Figure 3. HAM solutions for different fractional values of Susceptible class $S(t)$.

Table 4. Comparison of the HAM and RK4 solutions with NDSolve solution for $\alpha = 1$ of Infected class $I(t)$.

t	NDSolve	RK4	HAM	AE by RK4	AE by HAM
0	20	20	20	0	0
1	21.9450435	21.945044	21.9450438	5.3173×10^{-7}	3.3173×10^{-7}
2	23.7854755	23.785476	23.7854757	4.8949×10^{-7}	1.8949×10^{-7}
3	25.5265147	25.526515	25.5265148	3.2387×10^{-7}	1.2387×10^{-7}
4	27.1731599	27.173160	27.1731601	1.4838×10^{-7}	2.4838×10^{-7}
5	28.7301953	28.730195	28.7301956	3.1968×10^{-7}	2.8031×10^{-7}
6	30.2021953	30.202195	30.2021955	3.5782×10^{-7}	1.4217×10^{-7}
7	31.5935303	31.593530	31.5935305	3.3022×10^{-7}	1.6977×10^{-7}
8	32.9083727	32.908372	32.9083728	6.9206×10^{-7}	1.0793×10^{-7}
9	34.1507038	34.150703	34.1507035	7.7676×10^{-7}	2.7676×10^{-7}
10	35.3243184	35.324317	35.3243177	1.4162×10^{-6}	7.1620×10^{-7}

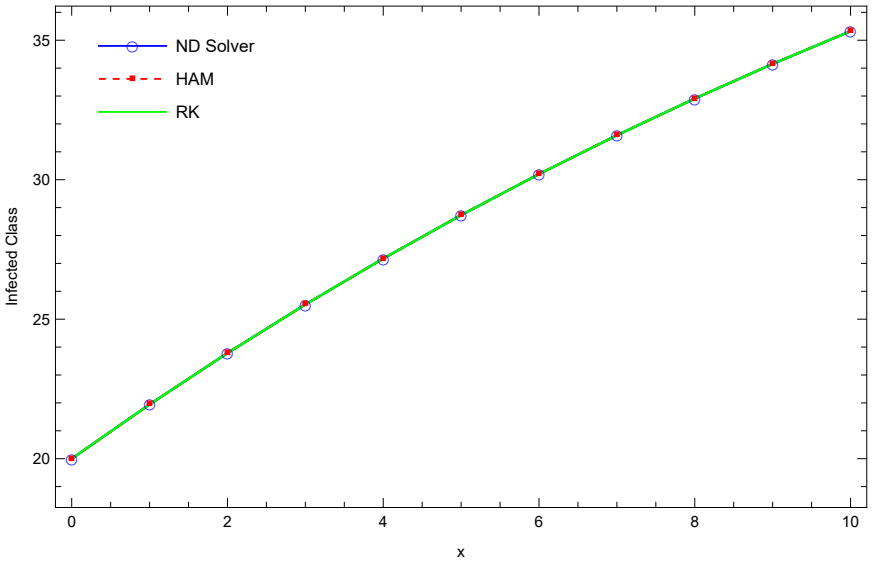

Figure 4. Comparison of the HAM and RK4 solutions with NDSolve solution for $\alpha = 1$ of Infected class $I(t)$.

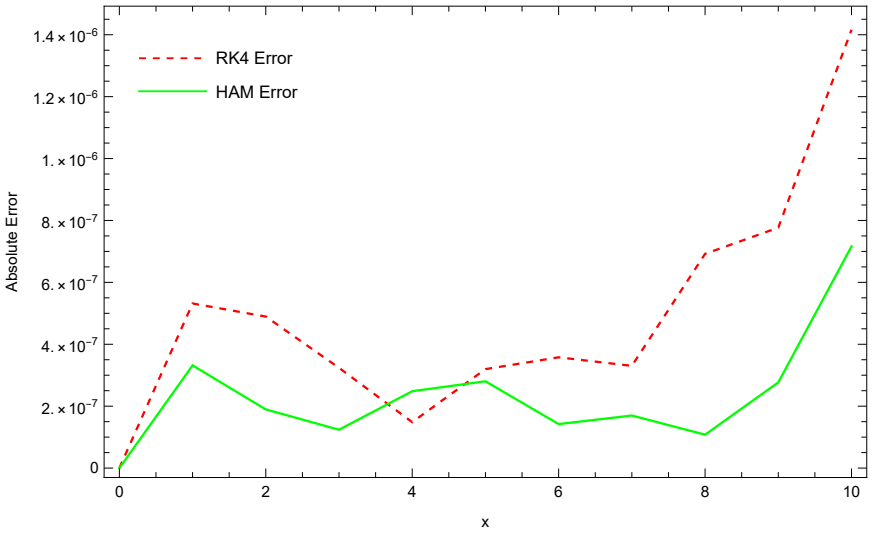

Figure 5. Error analysis of HAM and RK4 solution of Infected class $I(t)$.

Table 5. HAM solutions for different fractional values of Infected class $I(t)$.

t	$\alpha = 0.2$	$\alpha = 0.4$	$\alpha = 0.6$	$\alpha = 0.8$	$\alpha = 1$
0	20	20	20	20	20
1	22.0592782	22.1399004	22.1407625	22.0712908	21.9450438
2	22.3464469	22.7784712	23.1729573	23.5133872	23.7854757
3	22.5313407	23.2299783	23.9749521	24.7477457	25.5265148
4	22.6706221	23.5900178	24.6511673	25.8489143	27.1731601
5	22.7834905	23.8938424	25.2441114	26.8513599	28.7301956
6	22.8789473	24.1589307	25.7763446	27.7752266	30.2021955
7	22.9619840	24.3953946	26.2616296	28.6338326	31.5935305
8	23.0356752	24.6096797	26.7091316	29.4366901	32.9083728
9	23.1020573	24.8061794	27.1253358	30.1909623	34.1507035
10	23.1625527	24.9880397	27.5150401	30.9022565	35.3243177

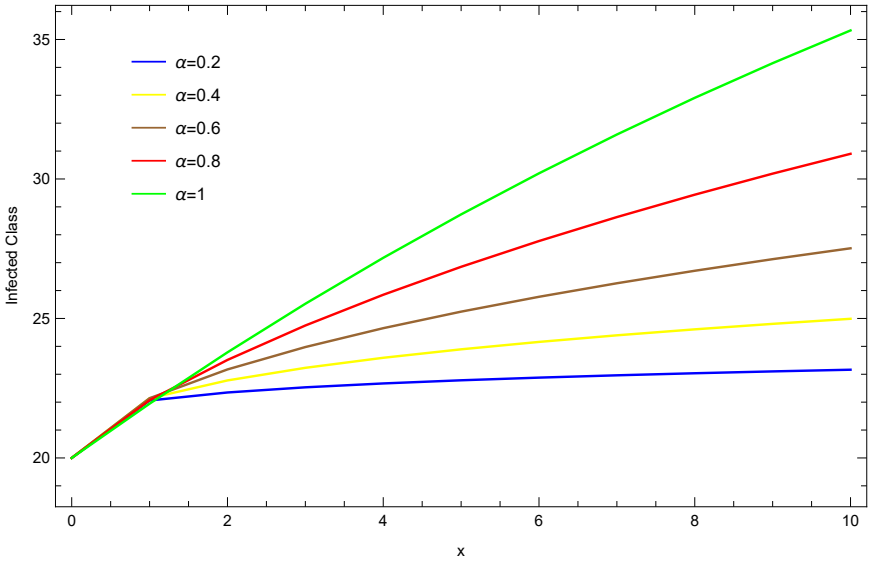

Figure 6. HAM solutions for different fractional values of Infected class $I(t)$.

Table 6. Comparison of the HAM and RK4 solutions with NDSolve solution for fractional value $\alpha = 1$ of Recovered class $R(t)$.

t	NDSolve	RK4	HAM	AE by RK4	AE by HAM
0	10	10	10	0	0
1	10.0470633	10.047065	10.0470629	1.7100×10^{-6}	3.8995×10^{-7}
2	10.1796394	10.179643	10.1796398	3.5837×10^{-6}	3.8375×10^{-7}
3	10.3847385	10.384743	10.3847393	4.4642×10^{-6}	7.6422×10^{-7}
4	10.6508497	10.650854	10.6508497	4.2776×10^{-6}	$2{,}2393\times10^{-8}$
5	10.9677881	10.967793	10.9677880	4.9150×10^{-6}	8.4973×10^{-7}
6	11.3265630	11.326569	11.3265631	6.0354×10^{-6}	1.3539×10^{-7}
7	11.7192523	11.719259	11.7192526	6.6798×10^{-6}	2.7981×10^{-7}
8	12.1388915	12.138898	12.1388915	6.4866×10^{-6}	1.3306×10^{-8}
9	12.5793696	12.579378	12.5793715	8.4285×10^{-6}	1.9285×10^{-6}
10	13.0353479	13.035357	13.0353511	9.1133×10^{-6}	3.2133×10^{-6}

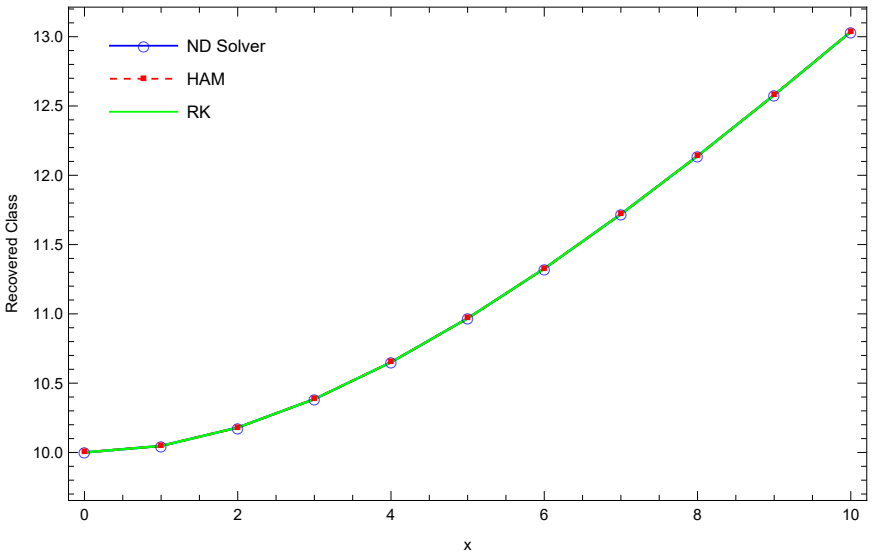

Figure 7. Comparison of the HAM and RK4 solutions with NDSolve solution for $\alpha = 1$ of Recovered class $R(t)$.

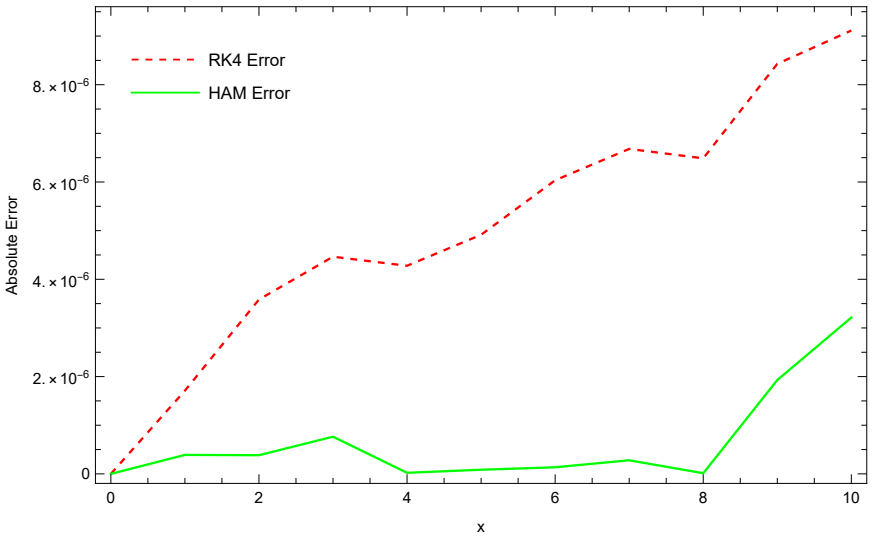

Figure 8. Error analysis of HAM and RK4 solution of Recovered class $R(t)$.

Table 7. HAM solutions for different fractional values of Recovered class $R(t)$.

t	$\alpha = 0.2$	$\alpha = 0.4$	$\alpha = 0.6$	$\alpha = 0.8$	$\alpha = 1$
0	10	10	10	10	10
1	10.0966724	10.0940005	10.0816155	10.0645163	10.0470629
2	10.1249458	10.1574912	10.1785762	10.1858362	10.1796398
3	10.1449803	10.2118510	10.2792078	10.3392375	10.3847393
4	10.1610094	10.2607256	10.3810004	10.5145169	10.6508497
5	10.1745848	10.3057359	10.4828629	10.7054924	10.9677880
6	10.1864729	10.3477937	10.5842227	10.9079347	11.3265631
7	10.1971161	10.3874810	10.6847509	11.1187588	11.7192526
8	10.2067956	10.4251993	10.7842497	11.3356244	12.1388915
9	10.2157028	10.4612416	10.8825980	11.5567097	12.5793715
10	10.2239745	10.4958302	10.9797229	11.7805708	13.0353511

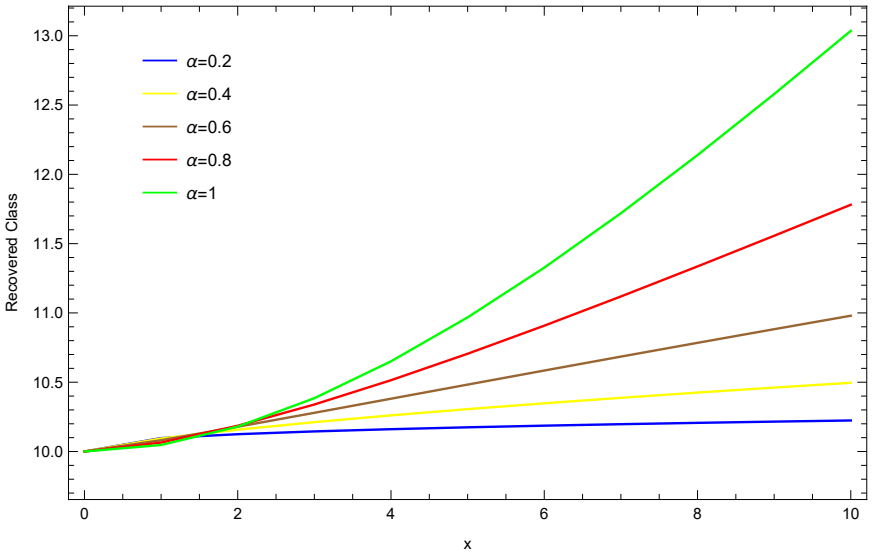

Figure 9. HAM solutions for different fractional values of Recovered class $R(t)$.

Table 8. Comparison of the HAM and RK4 solutions with NDSolve solution for $\alpha = 1$ of Listeria monocytogenes bacteria $L_c(t)$.

t	NDSolve	RK4	HAM	AE by RK4	AE by HAM
0	0.46051702	0.4605170186	0.46051702	1.1907×10^{-12}	1.1907×10^{-12}
1	0.44353680	0.443537	0.44353677	1.9655×10^{-7}	3.3445×10^{-8}
2	0.42791563	0.427916	0.42791561	3.7027×10^{-7}	1.9726×10^{-8}
3	0.41349734	0.413497	0.41349732	3.4210×10^{-7}	2.2100×10^{-8}
4	0.40014878	0.400149	0.40014878	2.1794×10^{-7}	2.0516×10^{-9}
5	0.38775579	0.387756	0.38775577	2.1016×10^{-7}	1.9833×10^{-8}
6	0.37621983	0.376220	0.37621981	1.7330×10^{-7}	1.6691×10^{-8}
7	0.36545549	0.365455	0.36545548	4.9216×10^{-7}	1.2163×10^{-8}
8	0.35538836	0.355388	0.35538835	3.5874×10^{-7}	8.7483×10^{-9}
9	0.34595327	0.345953	0.34595329	2.7430×10^{-7}	5.4302×10^{-8}
10	0.33709296	0.337093	0.33709313	4.3194×10^{-8}	1.7319×10^{-7}

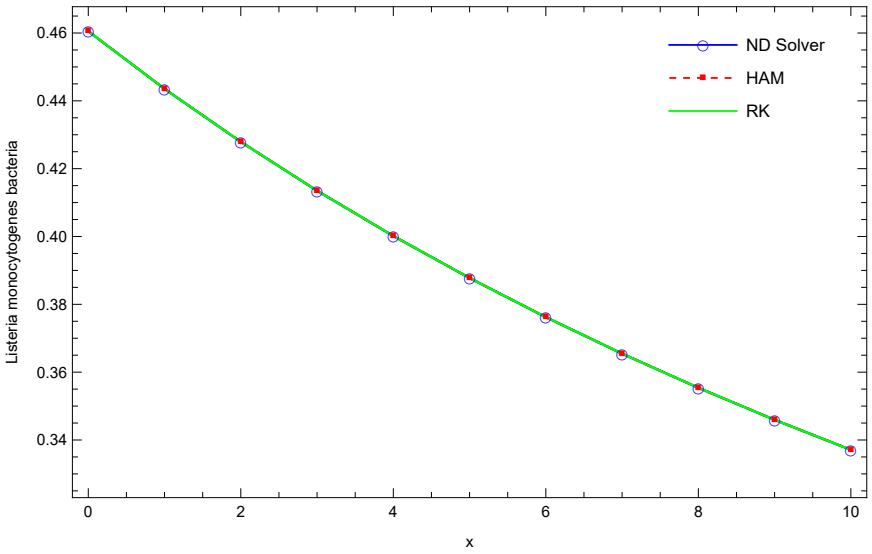

Figure 10. Comparison of the HAM and RK4 solutions with NDSolve solution for $\alpha = 1$ of Listeria monocytogenes bacteria $L_c(t)$.

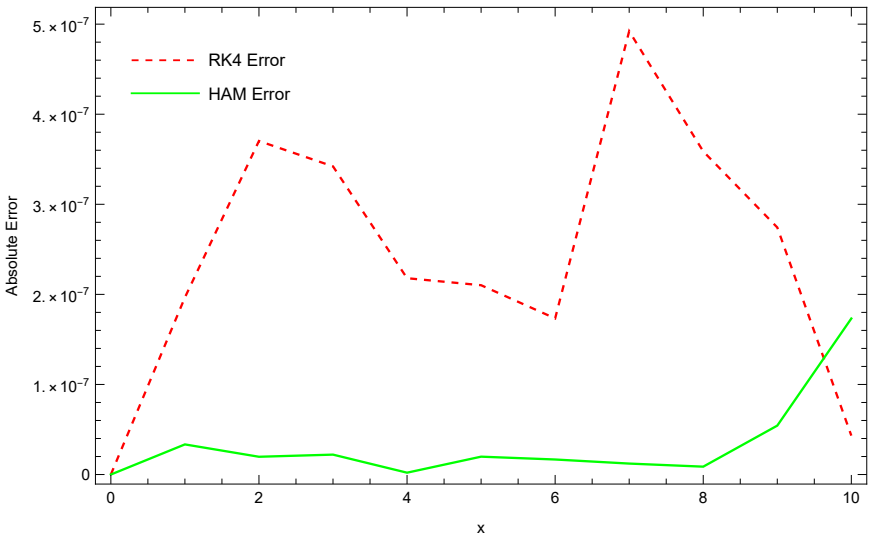

Figure 11. Error analysis of HAM and RK4 solution of Listeria monocytogenes bacteria $L_c(t)$.

Table 9. HAM solutions for different fractional values of Listeria monocytogenes bacteria $L_c(t)$.

t	$\alpha = 0.2$	$\alpha = 0.4$	$\alpha = 0.6$	$\alpha = 0.8$	$\alpha = 1$
0	0.46051702	0.46051702	0.46051702	0.46051702	0.46051702
1	0.44278681	0.44205854	0.44198586	0.44251107	0.44353677
2	0.44038893	0.43672803	0.43333953	0.43035900	0.42791561
3	0.43885365	0.43300260	0.42673634	0.42018102	0.41349732
4	0.43770144	0.43005630	0.42124074	0.41125905	0.40014878
5	0.43677040	0.42758616	0.41647245	0.40325486	0.38775577
6	0.43598482	0.42544256	0.41223023	0.3959690	0.37621981
7	0.43530280	0.42353928	0.40839177	0.38927004	0.36545548
8	0.43469858	0.42182152	0.40487600	0.38306462	0.35538835
9	0.43415512	0.42025205	0.40162590	0.37728451	0.34595329
10	0.43366052	0.41880426	0.39859958	0.37187872	0.33709313

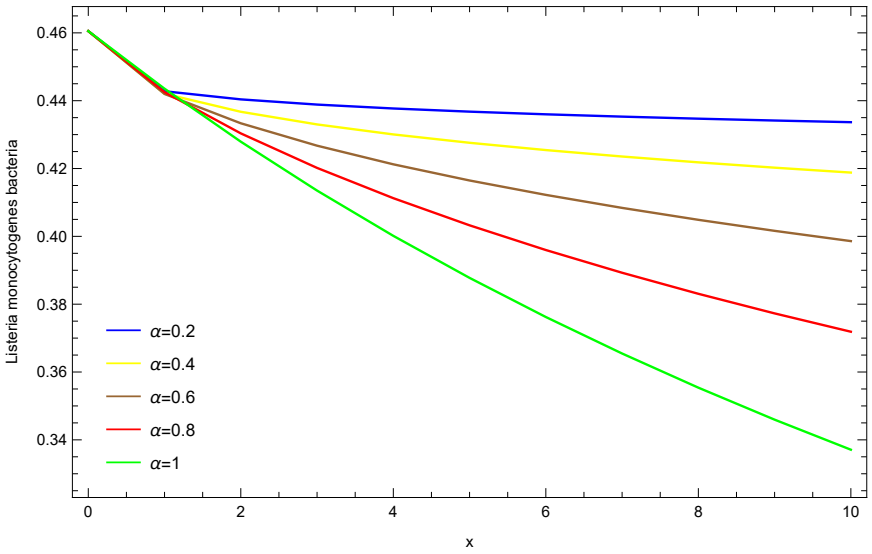

Figure 12. HAM solutions for different fractional values of Listeria monocytogenes bacteria $L_c(t)$.

Table 10. Comparison of the HAM and RK4 solutions with NDSolve solution for $\alpha = 1$ of Contaminated food $F_c(t)$.

t	NDSolve	RK4	HAM	AE by RK4	AE by HAM
0	300	300	300	0	0
1	297.1288075	297.070806	297.1288076	5.8001×10^{-2}	8.1392×10^{-8}
2	294.3144685	294.200785	294.3144687	1.1368×10^{-1}	1.5748×10^{-7}
3	291.5558572	291.388743	291.5558574	1.6711×10^{-1}	2.3338×10^{-7}
4	288.85187	288.633507	288.8518702	2.1836×10^{-1}	2.0144×10^{-7}
5	286.2014254	285.933931	286.2014256	2.6749×10^{-1}	1.6826×10^{-7}
6	283.6034632	283.288891	283.6034633	3.1457×10^{-1}	8.6948×10^{-8}
7	281.056944	280.697283	281.0569441	3.5966×10^{-1}	6.9443×10^{-8}
8	278.5608492	278.158029	278.5608494	4.0282×10^{-1}	1.6433×10^{-7}
9	276.1141787	275.670072	276.1141807	4.4410×10^{-1}	2.0355×10^{-6}
10	273.7159552	273.232375	273.7159592	4.8358×10^{-1}	3.9881×10^{-6}

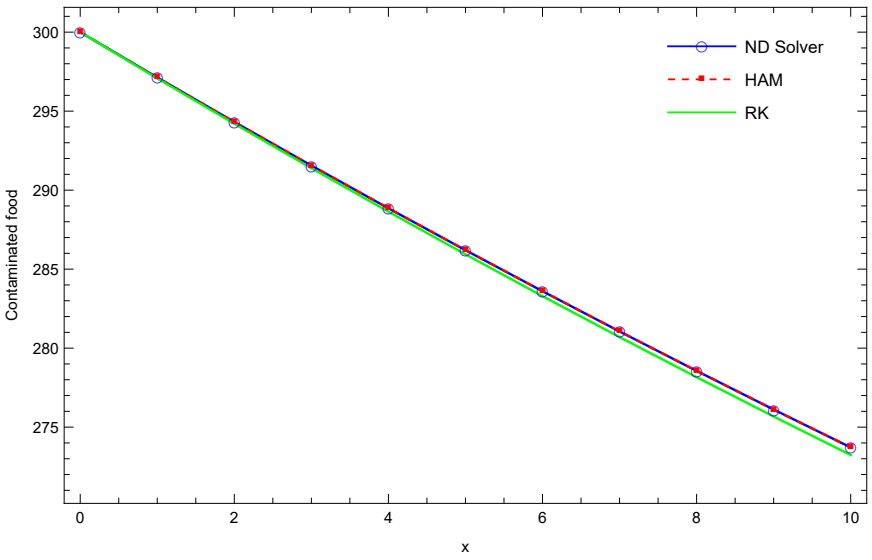

Figure 13. Comparison of the HAM and RK4 solutions with NDSolve solution for $\alpha = 1$ of Contaminated food $F_c(t)$.

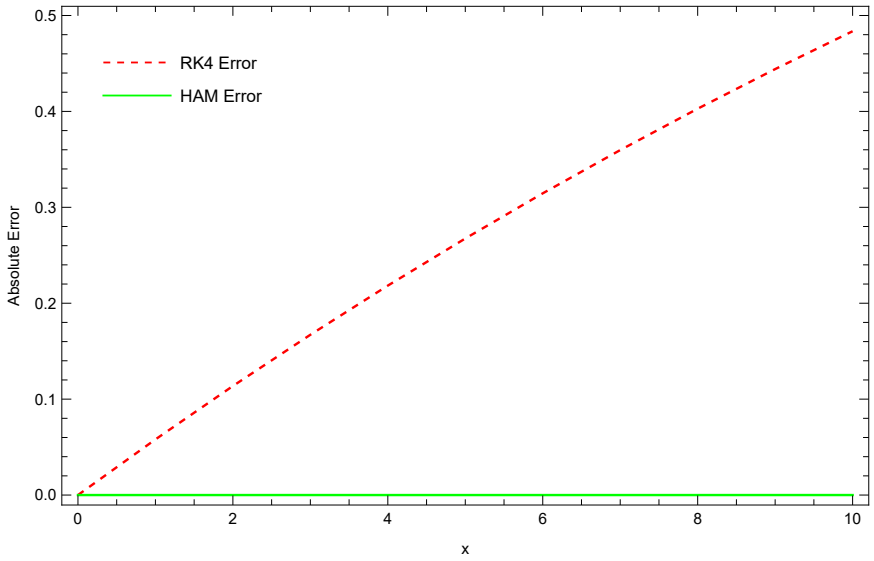

Figure 14. Error analysis of HAM and RK4 solution of Contaminated food $F_c(t)$.

Table 11. HAM solutions for different fractional values of Contaminated food $F_c(t)$.

t	$\alpha = 0.2$	$\alpha = 0.4$	$\alpha = 0.6$	$\alpha = 0.8$	$\alpha = 1$
0	300	300	300	300	300
1	296.9056349	296.7927607	296.8063494	296.9265373	297.1288076
2	296.4562115	295.7932738	295.1991475	294.6997852	294.3144687
3	296.1643999	295.0739555	293.9174875	292.7315919	291.5558574
4	295.9432920	294.4926186	292.8132151	290.9234188	288.8518702
5	295.7632970	293.9965691	291.8262975	289.2312394	286.2014256
6	295.6104932	293.5595786	290.9249801	287.6300724	283.6034633
7	295.4771393	293.1664221	290.0899411	286.1038309	281.0569441
8	295.3584554	292.8073652	289.3083395	284.6412933	278.5608494
9	295.2512696	292.4757548	288.5711040	283.2341864	276.1141807
10	295.1533620	292.1668141	287.8715310	281.8761571	273.7159592

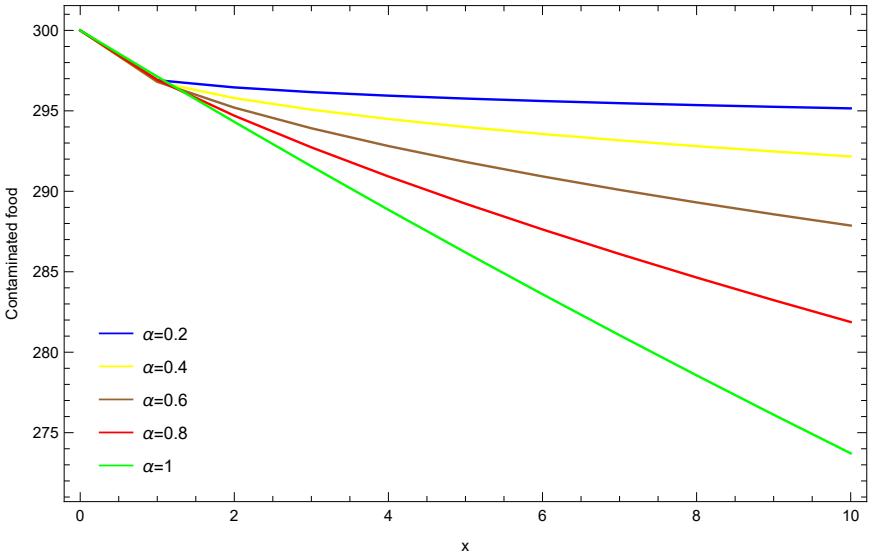

Figure 15. HAM solutions for different fractional values of Contaminated food $F_c(t)$.

Table 12. Comparison of the HAM and RK4 solutions with NDSolve solution for $\alpha = 1$ of uncontaminated food $F_u(t)$.

t	NDSolve	RK4	HAM	AE by RK4	AE by HAM
0	10	10	10	0	0
1	12.8711925	12.929194	12.8711924	5.8001×10^{-2}	8.1392×10^{-8}
2	15.6855315	15.799215	15.6855313	1.1368×10^{-1}	1.5748×10^{-7}
3	18.4441428	18.611257	18.4441426	1.6711×10^{-1}	2.3338×10^{-7}
4	21.1481300	21.366493	21.1481298	2.1836×10^{-1}	2.0144×10^{-7}
5	23.7985746	24.066069	23.7985744	2.6749×10^{-1}	1.6826×10^{-7}
6	26.3965368	26.711109	26.3965367	3.1457×10^{-1}	8.6948×10^{-8}
7	28.9430560	29.302717	28.9430559	3.5966×10^{-1}	6.9443×10^{-8}
8	31.4391508	31.841971	31.4391506	4.0282×10^{-1}	1.6433×10^{-7}
9	33.8858213	34.329928	33.8858194	4.4410×10^{-1}	1.9355×10^{-6}
10	36.2840448	36.767625	36.2840408	4.8358×10^{-1}	3.9881×10^{-6}

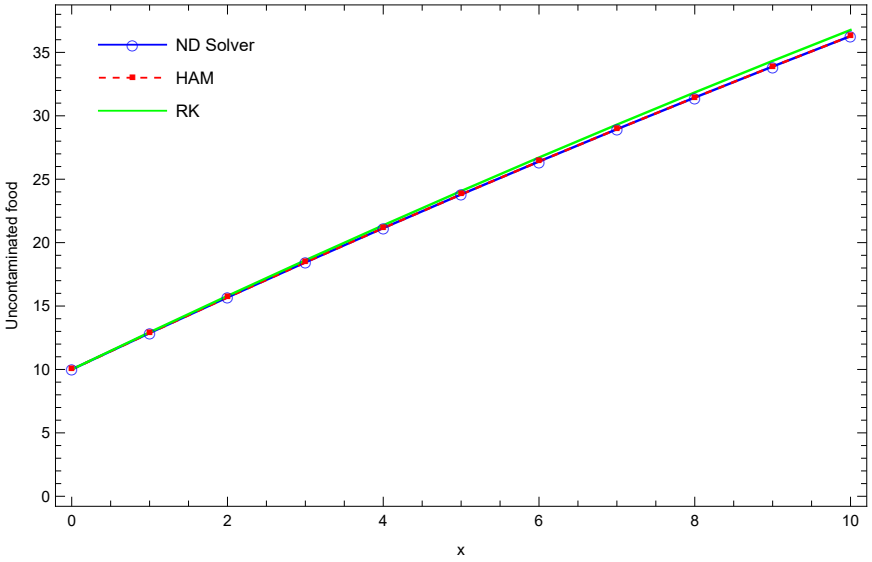

Figure 16. Comparison of the HAM and RK4 solutions with NDSolve solution for $\alpha = 1$ of uncontaminated food $F_u(t)$.

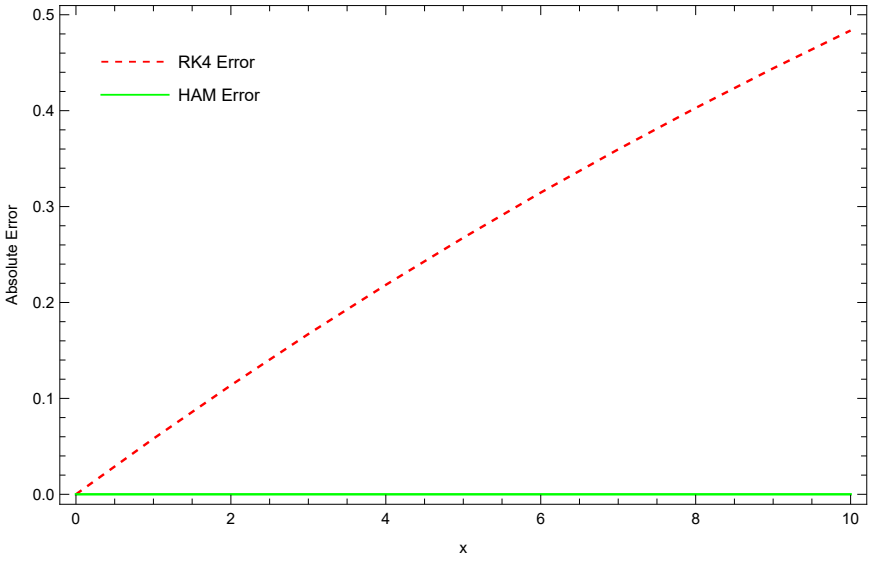

Figure 17. Error analysis of HAM and RK4 solution of uncontaminated food $F_u(t)$.

Table 13. HAM solutions for different fractional values of uncontaminated food $F_u(t)$.

t	$\alpha = 0.2$	$\alpha = 0.4$	$\alpha = 0.6$	$\alpha = 0.8$	$\alpha = 1$
0	10	10	10	10	10
1	13.0943651	13.2072393	13.1936506	13.0734627	12.8711924
2	13.5437885	14.2067262	14.8008525	15.3002148	15.6855313
3	13.8356001	14.9260445	16.0825125	17.2684081	18.4441426
4	14.0567080	15.5073814	17.1867849	19.0765812	21.1481298
5	14.2367030	16.0034310	18.1737025	20.7687606	23.7985744
6	14.3895068	16.4404214	19.0750199	22.3699276	26.3965367
7	14.5228607	16.8335780	19.9100589	23.8961691	28.9430559
8	14.6415446	17.1926348	20.6916605	25.3587067	31.4391506
9	14.7487304	17.5242452	21.4288960	26.7658136	33.8858194
10	14.8466380	17.8331859	22.1284690	28.1238430	36.2840408

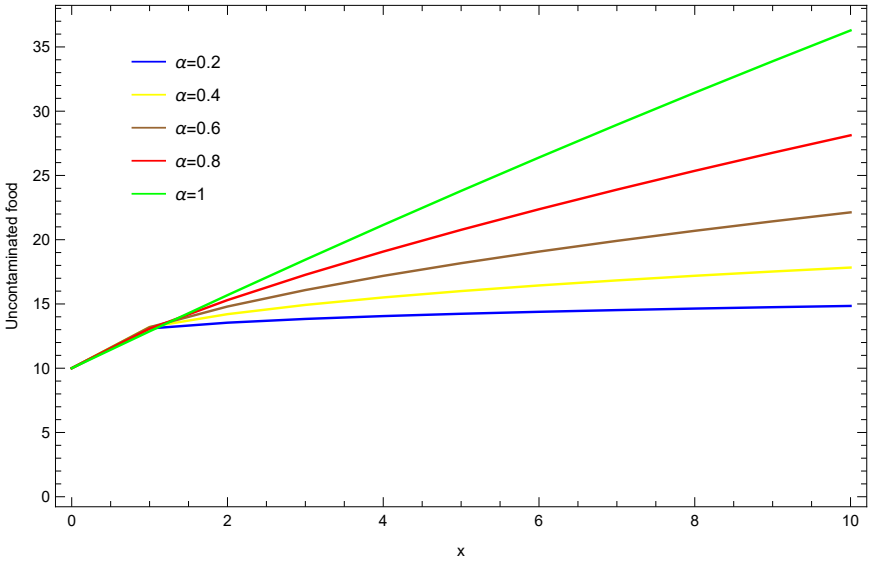

Figure 18. HAM solutions for different fractional values of uncontaminated food $F_u(t)$.

7. Conclusion

In this manuscript, we examined the Listeria infection model using two distinct approaches, namely the HAM and RK4 methodologies. Here, we studied the effects of various parameters while doing a practical analysis of susceptible, infected, recovered class, Listeria monocytogenes bacteria, contaminated food, and uncontaminated food. The semi-analytical method, HAM, produces the semi-analytical solution of a given model following additional deformations; the outcomes are compared to the solutions obtained using the NDSolver and RK4 methods. According to this study, HAM offers solutions with a higher accuracy than the RK4 numerical method. The tables and graphs demonstrate that the HAM is effective, straightforward, computationally appealing, and requires less computer time. Additionally, analyzing the solution of a system of ODEs offers insights for future research on more complex equations. The slight modification in the method is recommended to be extended to a system of higher-order ODEs, a system of fractional partial differential equations, and delay differential equations.

Acknowledgements

The author expresses his affectionate thanks to the DST-SERB, Govt. of India, New Delhi, for the financial support under Empowerment and Equity Opportunities for Excellence in Science for 2023-2026. F.No.EEQ/2022/620 Dated:07/02/2023.

References

[1] K. Srinivasa, M. Mulimani and W. Adel, *A numerical approach for solving nonlinear fractional Klein-Gordon equation with applications in quantum mechanics*, Journal of Nonlinear, Complex and Data Science, 2024, 25(2), 173–195.

[2] S. Kumbinarasaiah and M. Mulimani, *Fibonacci wavelets-based numerical method for solving fractional order (1+1)-dimensional dispersive partial differential equation*, International Journal of Dynamics and Control, 2023, 11(5), 2232–2255.

[3] E. T. Ryser and E. H. Marth, *Listeria, listeriosis, and food safety*, CRC Press, Boca Raton, 2007.

[4] C. Shi, D. Lv, K. Zhou, T. Jin, G. Wang, B. Wang, Y. Li and Y. Xu, *Clinical and laboratory characteristics of patients infected by Listeria monocytogenes at a tertiary hospital in Hefei City, China*, Infection and Drug Resistance, 2021, 14, 4409–4419.

[5] J. A. Lepe, *Current aspects of listeriosis*, Medicina Clínica, 2020, 154(11), 453–458.

[6] F. Duarte, S. M. Pinto, A. C. Trigo, F. Guimaraes, R. Pereira, M. Neno, R. C. de Abreu and I. Neves, *A rare presentation of Listeria monocytogenes infection: perianal abscess associated with lumbar spine osteitis*, IDCases, 2019, 15, e00488.

[7] S. T. Duze, M. Marimani and M. Patel, *Tolerance of Listeria monocytogenes to biocides used in food processing environments*, Food Microbiology, 2021, 97, 103758.

[8] B. Giménez, N. Graiver, L. Giannuzzi and N. Zaritzky, *Treatment of beef with gaseous ozone: Physicochemical aspects and antimicrobial effects on heterotrophic microflora and Listeria monocytogenes*, Food Control, 2021, 121, 107602.

[9] S. H. Roh, Y. J. Oh, S. Y. Lee, J. H. Kang and S. C. Min, *Inactivation of Escherichia coli O157: H7, Salmonella, Listeria monocytogenes, and Tulane virus in processed chicken breast via atmospheric in-package cold plasma treatment*, Lwt, 2020, 127, 109429.

[10] J. K. Asamoah, E. Addai, Y. D. Arthur and E. Okyere, *A fractional mathematical model for listeriosis infection using two kernels*, Decision Analytics Journal, 2023, 6, 100191.

[11] A. G. Massia, D. A. Laroque, J. O. de Moraes, S. Heidtmann, D. T. Buosi and B. A. Carciofi, *Prior freezing impact on the growth kinetics of Listeria monocytogenes in hot dog sausages*, Food Control, 2024, 157, 110186.

[12] L. Zhang, V. R. Parreira, A. Rahman, B. A. Smith, D. S. Munther and J. M. Farber, *Survival and predictive modeling of Listeria monocytogenes under simulated human gastric conditions in the presence of bovine milk products*, International Journal of Food Microbiology, 2023, 396, 110201.

[13] S. Banerjee, *Mathematical modeling: models, analysis and applications*, Chapman and Hall/CRC, New York, 2021.

[14] L. Ait Mahiout, N. Bessonov, B. Kazmierczak and V. Volpert, *Mathematical modeling of respiratory viral infection and applications to SARS-CoV-2 progression*, Mathematical Methods in the Applied Sciences, 2023, 46(2), 1740–1751.

[15] A. Aghsami, S. R. Abazari, A. Bakhshi, M. A. Yazdani, S. Jolai and F. Jolai, *A meta-heuristic optimization for a novel mathematical model for minimizing costs and maximizing donor satisfaction in blood supply chains with finite capacity queueing systems*, Healthcare Analytics, 2023, 3, 100136.

[16] R. A. Pearson, S. G. Wicha and M. Okour, *Drug combination modeling: methods and applications in drug development*, The Journal of Clinical Pharmacology, 2023, 63(2), 151–165.

[17] G. Ledder, *Mathematical modeling for epidemiology and ecology*, Springer, Switzerland, 2023.

[18] M. Yang, J. Meng, L. Han, X. Yu, Z. Fan and Y. Yuan, *Pharmacokinetic study of triptolide nanocarrier in transdermal drug delivery system—Combination of experiment and mathematical modeling*, Molecules, 2023, 28(2), 553.

[19] S. S. Tuly, M. Mahiuddin and A. Karim, *Mathematical modeling of nutritional, color, texture, and microbial activity changes in fruit and vegetables during drying: A critical review*, Critical Reviews in Food Science and Nutrition, 2023, 63(13), 1877–1900.

[20] S. Khirsariya, S. Rao and J. Chauhan, *Semi-analytic solution of time-fractional Korteweg-de Vries equation using fractional residual power series method*, Results in Nonlinear Analysis, 2022, 5(3), 222–234.

[21] J. P. Chauhan and S. R. Khirsariya, *A semi-analytic method to solve nonlinear differential equations with arbitrary order*, Results in Control and Optimization, 2023, 12, 100267.

[22] S. R. Khirsariya and S. B. Rao, *On the semi-analytic technique to deal with nonlinear fractional differential equations*, Journal of Applied Mathematics and Computational Mechanics, 2023, 22(1), 13–26.

[23] Q. Chen, Z. Sabir, M. A. Raja, W. Gao and H. M. Baskonus, *A fractional study based on the economic and environmental mathematical model*, Alexandria Engineering Journal, 2023, 65, 761–770.

[24] K. Mukdasai, Z. Sabir, M. A. Raja, P. Singkibud, R. Sadat and M. R. Ali, *A computational supervised neural network procedure for the fractional SIQ mathematical model*, The European Physical Journal Special Topics, 2023, 232(5), 535–546.

[25] P. Veeresha and L. Akinyemi, *Fractional approach for mathematical model of Phytoplankton-toxic Phytoplankton-Zooplankton system with Mittag-Leffler kernel*, International Journal of Biomathematics, 2023, 16(03), 2250090.

[26] H. Bilgil, A. Yousef, A. Erciyes, Ü. Erdinç and Z. Öztürk, *A fractional-order mathematical model based on vaccinated and infected compartments of SARS-CoV-2 with a real case study during the last stages of the epidemiological event*, Journal of computational and applied mathematics, 2023, 425, 115015.

[27] S. R. Khirsariya, S. B. Rao and G. S. Hathiwala, *Investigation of fractional diabetes model involving glucose-insulin alliance scheme*, International Journal of Dynamics and Control, 2024, 12(1), 1–14.

[28] S. R. Khirsariya, J. P. Chauhan and G. S. Hathiwala, *Study of fractional diabetes model with and without complication class*, Results in Control and Optimization, 2023, 12, 100283.

[29] E. Addai, L. Zhang, J. K. Asamoah and J. F. Essel, *A fractional order age-specific smoke epidemic model*, Applied Mathematical Modelling, 2023, 119, 99–118.

[30] S. Sharma, P. Goswami, D. Baleanu and R. S. Dubey, *Comprehending the model of omicron variant using fractional derivatives*, Applied Mathematics in Science and Engineering, 2023, 31(1), 2159027.

[31] K. N. Sachin, K. Suguntha Devi and S. Kumbinarasaiah, *A semi-analytic and numerical approach to the fractional differential equations*, Iranian Journal of Numerical Analysis and Optimization, 2024, 14(4), 1069–1105.

[32] L. Morrow and M. Simpson, *An Investigation of the Homotopy Analysis Method for solving non-linear differential equations*, Australian Mathematical Science Institute, Melbourne, 2014.

[33] S. J. Liao, *Homotopy Analysis Method in Non-linear differential equations*, Springer, Heidelberg, 2012.

[34] Z. M. Odibat, *A study on the convergence of homotopy analysis method*, Applied Mathematics and Computation, 2010, 217(2), 782–789.

[35] S. Kumbinarasaiah and M. P. Preetham, *A study on homotopy analysis method and clique polynomial method*, Computational Methods for Differential Equations, 2022, 10(3), 774–788.

[36] S. Liao, *Advances in the homotopy analysis method*, World Scientific, Singapore, 2013.

[37] M. Zurigat, S. Momani, Z. Odibat and A. Alawneh, *The homotopy analysis method for handling systems of fractional differential equations*, Applied Mathematical Modelling, 2010, 34(1), 24–35.

[38] M. Mulimani and S. Kumbinarasaiah, *Numerical solution for a fractional operator-based mathematical model of a brain tumour*, The Journal of Analysis, 2024. DOI: 10.1007/s41478-024-00769-6

[39] K. N. Sachin, K. Suguntha Devi and S. Kumbinarasaiah, *A study on the Fractional Ebola Virus Model by the semi-analytic and numerical approach*, Computational Methods for Differential Equations, 2024.
DOI: 10.22034/cmde.2024.61485.2653

[40] S. Liao, *Beyond perturbation: introduction to the homotopy analysis method*, CRC press, New York, 2003.

[41] S. Liao, *Notes on the homotopy analysis method: some definitions and theorems*. Communications in Nonlinear Science and Numerical Simulation. 2009, 14(4), 983–997.

[42] J. P. Chauhan, S. R. Khirsariya, B. M. Yeolekar and M. A. Yeolekar, *Fractional mathematical model of Listeria infection caused by pre-cooked package food*, Results in Control and Optimization, 2024, 14, 100371.